

Thermal Decomposition of Isopropyl Nitrate: Kinetics and Products.

Julien Morin and Yuri Bedjanian*

Institut de Combustion, Aérothermique, Réactivité et Environnement (ICARE), CNRS and Université
d'Orléans, 45071 Orléans Cedex 2, France

* To whom correspondence should be addressed. Tel.: +33 238255474, Fax: +33 238696004, e-mail:
yuri.bedjanian@cnrs-orleans.fr

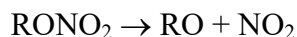
ABSTRACT

Kinetics and products of the thermal decomposition of isopropyl nitrate (IPN, $C_3H_7NO_3$) have been studied using a low pressure flow reactor combined with a quadrupole mass spectrometer. The rate constant of IPN decomposition was measured as a function of pressure (1 -12.5 Torr of helium) and temperature in the range 473 – 658 K using two methods: from kinetics of nitrate loss and those of reaction product (CH_3 radical) formation. The fit of the observed falloff curves with two parameter expression $k_1 = \frac{k_0 k_\infty [M]}{k_0 [M] + k_\infty} \times 0.6^{(1 + (\log(\frac{k_0 [M]}{k_\infty}))^2)^{-1}}$ provided the following low and high pressure limits for the rate constant of IPN decomposition: $k_0 = 6.60 \times 10^{-5} \exp(-15190/T) \text{ cm}^3 \text{ molecule}^{-1} \text{ s}^{-1}$ and $k_\infty = 1.05 \times 10^{16} \exp(-19850/T) \text{ s}^{-1}$, respectively, which allow to determine (via above expression) the values of k_1 (with 20% uncertainty) in the temperature and pressure range of the study. It was observed that thermal decomposition of IPN proceeds through initial breaking of the O–NO₂ bond leading to formation of NO₂ and isopropoxy radical (CH₃)₂CHO, which rapidly decomposes forming CH₃ and acetaldehyde as final products. The yields of NO₂, CH₃ and acetaldehyde upon decomposition of isopropyl nitrate were measured to be (0.98 ± 0.15), (0.96 ± 0.14) and (0.99 ± 0.15), respectively. In addition, the kinetic data were used to determine the O-NO₂ bond dissociation energy in isopropyl nitrate, 38.2 ± 4.0 kcal mol⁻¹.

1. INTRODUCTION

Organic nitrates are important species in atmospheric and combustion chemistry. In the atmosphere, organic nitrates are formed in addition reaction of peroxy radicals with NO and also in the NO₃-initiated oxidation of unsaturated organic compounds.¹ They are considered as stable species with lifetimes of several days or weeks (depending on their photolysis rate and reactivity toward OH radicals),² behaving as reservoirs for reactive nitrogen. In combustion processes, nitrates, used as fuel additives, are known to promote the ignition of diesel fuel. Production of chain-initiating radicals and, possibly, the heat released during nitrate decomposition in the pre-ignition phase are thought to decrease the ignition-delay time.³⁻⁵

Thermal decomposition of acyclic nitrates is supposed to proceed through a radical mechanism with initial dissociation of the O–NO₂ bond leading to formation of NO₂ and alkoxy radical (RO):



The alkoxy radicals can undergo a number of competing reaction pathways, including unimolecular decomposition at relatively high temperatures, which usually occurs through C–C bond fission to produce a carbonyl compound, and a unimolecular isomerization, which generates a hydroxy-substituted alkyl radical.⁶

Available quantitative information on the rate constants and products of thermal decomposition of nitrates in the gas phase is very limited.⁷⁻¹⁵ In the present work, we report the results of kinetic (measurements of the rate constant as a function of pressure and temperature) and mechanistic (identification and quantification of the reaction products including those of isopropoxy radical decomposition) study of the thermal decomposition of isopropyl nitrate (IPN):



2. EXPERIMENTAL

Thermal decomposition of isopropyl nitrate was studied at total pressure of helium between 1 and 12.5 Torr and in the temperature range (473 - 658) K. Experiments were carried out in a flow reactor under laminar flow conditions. Modulated molecular beam mass spectrometer with electron impact ionization was used to monitor IPN and its dissociation products. The flow reactor (Figure 1) developed recently for kinetic studies at elevated temperatures (up to 1000K) consisted of a Quartz tube with an electrical heater and water-cooled extremities.¹⁶ Temperature in the reactor was measured with a *K*-type thermocouple positioned in the middle of the reactor in contact with its outer surface. Temperature gradients along the flow tube measured with a thermocouple inserted in the reactor through the movable injector was less than 1%.¹⁶

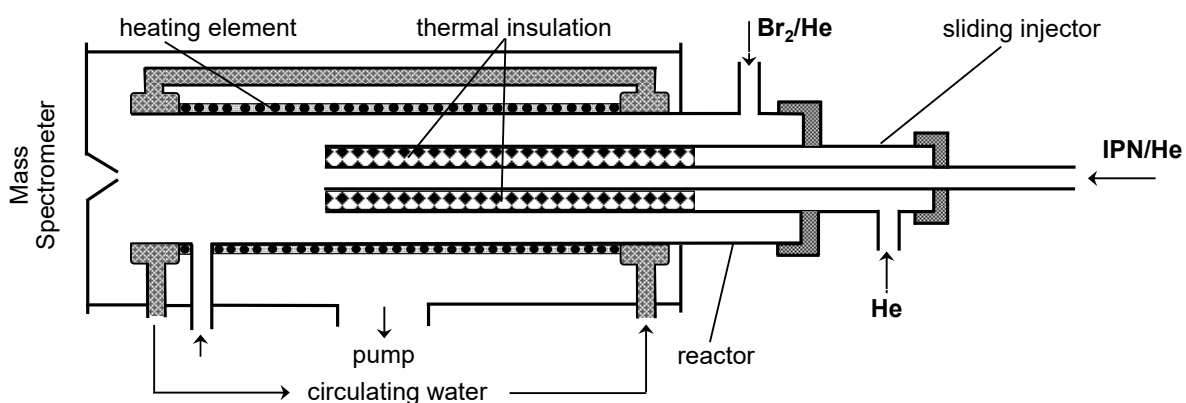


Figure 1. Diagram of the flow reactor.

Isopropyl nitrate was introduced into the flow reactor from a 10L flask containing IPN/He mixture through movable injector that allowed to vary its residence time in the reactor. The inner tube of the injector, through which nitrate was supplied, was thermally insulated in order to minimize the possible decomposition of IPN inside (Figure 1). IPN was detected by mass spectrometry at its fragment peak at $m/z = 90$ ($\text{CH}_3\text{CHONO}_2^+$), which is much more intensive than that of the parent ion ($m/z = 105$). CH_3 radicals were detected as CH_3Br at $m/z = 94/96$ (CH_3Br^+) after being scavenged by an excess of Br_2 via reaction:



$$k_2 = 2.0 \times 10^{-11} \exp(197/T) \text{ cm}^3 \text{ molecule}^{-1} \text{ s}^{-1} \quad (T = 296-532\text{K})^{17}$$

All other species were detected at their parent peaks: $m/z = 44$ (acetaldehyde, CH_3CHO^+), 160 (Br_2^+), 46 (NO_2^+). The absolute concentrations of all the species in the reactor were calculated from their flow rates obtained from the measurements of the pressure drop of mixtures of the species with helium in calibrated volume flasks.

The purities and origin of the gases used were as follows: He >99.9995% (Alphagaz); IPN >99.0% (Sigma-Aldrich) was degassed before use; Br_2 >99.99% (Aldrich); NO_2 > 99% (Alphagaz); acetaldehyde > 99.5% (Sigma-Aldrich).

3. RESULTS AND DISCUSSION

The rate constant of reaction (1) was measured in the temperature range $T = 473 - 658$ K as a function of total pressure of He (used as a carrier gas in all experiments) between 1 and 12.5 Torr. We have employed two methods for the measurements of the rate of nitrate decomposition. The first one, used at higher temperatures ($T = 563 - 658\text{K}$) consisted in a direct monitoring of the kinetics of nitrate loss. In the second approach the rate constant of the nitrate decomposition was determined from the kinetics of product formation (CH_3 radical) under conditions where consumption of nitrate was negligible ($T = 473-565\text{K}$).

3.1. Rate constant of reaction (1) from kinetics of IPN decomposition. In this series of experiments the rate constant of reaction (1) was determined in the temperature range 563 - 658 K from kinetics of isopropyl nitrate loss due to its decomposition. Flow velocity in the reactor was varied in the range (120 - 2520) cm s^{-1} , depending on the rate of IPN decomposition (i.e. depending on pressure and temperature), providing the maximum reaction time from 8 to 200 ms. It was observed that, at a given total pressure, consumption of nitrate

follows first order kinetics: $d[\text{IPN}]/dt = -k_1[\text{IPN}]$. Example of the exponential decays of IPN observed at different pressures in the reactor at $T = 630\text{K}$ is shown in Figure 2.

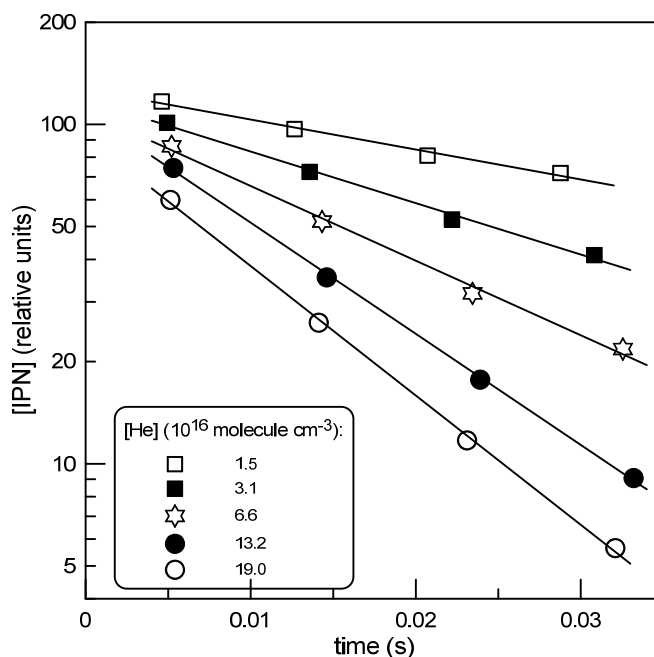


Figure 2. Example of kinetics of IPN decomposition at different pressures of He in the reactor: $T = 630\text{ K}$.

The values of k_1 (in s^{-1}) determined from the kinetics of IPN loss in Figure 2 are plotted in Figure 3 as a function of total pressure in the reactor. The uncertainty on the measurements of k_1 was estimated to be nearly 10%, including statistical error (within a few percent) and those on the measurements of the flows (5%), pressure (2%) and temperature (1%). One can note that in the pressure range of the present study, decomposition of the nitrate proceeds in the “falloff regime” (Figure 3). Generally the dependence of the rate constant on pressure in falloff regime is described using the Lindemann-Hinshelwood reaction scheme:



with addition of a broadening factor, F , to the Lindemann-Hinshelwood expressions, leading to¹⁸⁻¹⁹

$$k = \frac{k_0 k_\infty [M]}{k_0 [M] + k_\infty} F = k_0 [M] \left(\frac{1}{1 + k_0 [M] / k_\infty} \right) F \quad (\text{I})$$

where $k_0 = k_3$ and $k_\infty = k_3 k_4 / k_{-3}$ are low and high pressure limits of the rate constant, respectively, and the broadening factor F is determined as:

$$\log F \cong \frac{\log F_c}{1 + \left(\frac{\log(k_0 [M] / k_\infty)}{N} \right)^2} \quad (\text{II})$$

with $N = 0.75 - 1.27 \log F_c$.¹⁸⁻¹⁹

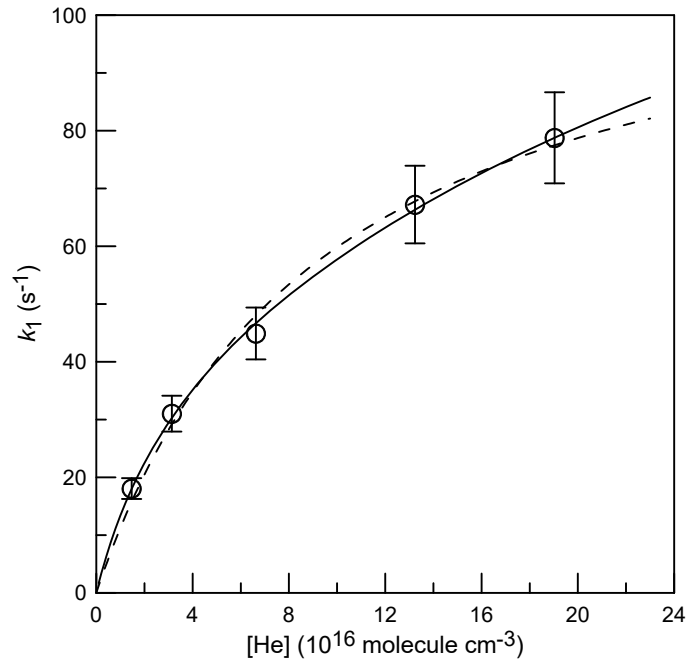


Figure 3. Rate of IPN decomposition as a function of total pressure of He in the reactor: T = 630 K, error bars correspond to 10% uncertainty on k_1 . Continuous line: fit according to equations (I) and (II) with fixed and independent of temperature $F_c = 0.6$; dashed line: fit according to equation (I) with $F = 1$.

So the falloff curve is characterized by three parameters, k_0 , k_∞ and F_c (called “center broadening factor”), all being reaction- and temperature-dependent. In practice, it is impossible to fit a limited part of falloff curve, usually determined in experiments, with three variable parameters. In the present study, in order to describe the dependence of the rate constant on pressure we adopted simplified approach used in JPL evaluation of kinetic data:²⁰ the experimental falloff curve was fitted accordingly to equation (I) with fixed and

independent of temperature $F_c = 0.6$ and $N \approx 1$ and two varied parameters, k_0 and k_∞ . Obviously, k_0 and k_∞ determined in this way depend on the choice of F_c -value, nevertheless this procedure allows to describe the experimental data with the three clearly specified parameters.

The continuous line in Figure 3 represents the fit to experimental data according to equations (I) and (II) with $F_c = 0.6$, $k_0 = 1.9 \times 10^{-15} \text{ cm}^3 \text{ molecule}^{-1} \text{ s}^{-1}$ and $k_\infty = 200.8 \text{ s}^{-1}$. It can be noted that fit to the experimental data according to Lindemann-Hinshelwood expression (expression (I) with $F = 1$, dashed line in Figure 3) also describes well the observed falloff curve, however with the values of k_0 and k_∞ lower by a factor 1.5 and 1.7, respectively. A similar procedure was applied for the determination of k_0 and k_∞ from the falloff curves observed at other temperatures (Figure 4). The results obtained in this way for k_0 and k_∞ are presented in Table 1.

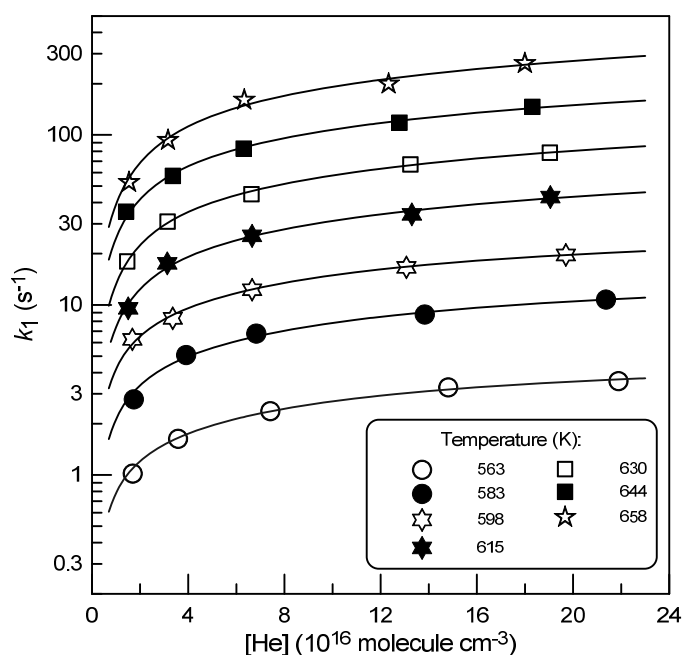


Figure 4. Rate of IPN decomposition as a function of total pressure of He measured at different temperatures from kinetics of IPN loss. Uncertainty on k_1 (nearly 10%) corresponds to the size of symbols. Continuous lines represent the best fit to the experimental data according to equations (I) and (II) with $F_c = 0.6$ and two varied parameters, k_0 and k_∞ .

Table 1. Thermal decomposition of IPN: summary of the measurements of k_0 and k_∞ .

T (K)	k_0 (10^{-16} cm ³ molecule ⁻¹ s ⁻¹) ^a	k_∞ (s ⁻¹) ^a	Method ^b
658	50.7	838	IPN kinetics
644	34.8	372	IPN kinetics
630	18.6	201	IPN kinetics
615	10.6	102	IPN kinetics
598	7.02	36.5	IPN kinetics
583	3.44	20.5	IPN kinetics
565	1.84	5.75	CH ₃ kinetics
563	1.35	6.26	IPN kinetics
546	0.70	1.54	CH ₃ kinetics
524	0.15	0.441	CH ₃ kinetics
507	0.054	0.101	CH ₃ kinetics
495	0.033	0.034	CH ₃ kinetics
473	0.0057	0.0060	CH ₃ kinetics

^a Estimated uncertainty factor of 1.5. ^b See text.

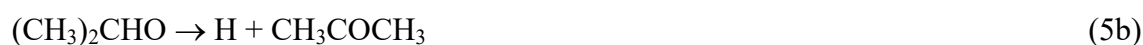
All the measurements described above were carried out with initial concentration of IPN of nearly 2×10^{12} molecule cm⁻³. In a special series of experiments carried out at $P = 9$ torr and $T = 580$ K we have verified for the possible dependence of the measured IPN decomposition rate on initial concentration of the nitrate. The rate of IPN decomposition was found to be independent (within 5%) of $[\text{IPN}]_0$ (Figure 1S, supporting Information), the last being varied in the range $(0.9 - 9.0) \times 10^{12}$ molecule cm⁻³.

Heterogeneous decomposition of IPN could potentially impact the measured loss rate of the nitrate. The best check for the presence of heterogeneous reaction is to carry out measurements with different surface to volume ratios in the reactor. This kind of experiments has been conducted by Adams & Bawn⁷ in their study of ethyl nitrate decomposition under static conditions. The authors have reported that a 7.4 times increase in surface of a Pyrex reaction vessel had no influence on the reaction rate at $T = 456$ K. Based on these results, a negligible (compared with homogeneous process) heterogeneous decomposition of IPN can be expected in our fast flow quartz reactor. In the present study, wall decomposition was not tested and assumed to be negligible.

3.2. Products of IPN decomposition. Thermal decomposition of isopropyl nitrate is expected to proceed through initial dissociation of the O–NO₂ bond leading to formation of NO₂ and isopropoxy radical:



The isopropoxy radicals can undergo unimolecular decomposition through the following two competitive reaction pathways:⁶



With the rate constants for reactions (5a) and (5b) calculated using microscopic reversibility by Curran,⁶ in the temperature range of the present study: (i) channel (5a) is highly dominant ($k_{5a}/k_{5b} = 200 - 800$), (ii) decomposition of (CH₃)₂CHO is instantaneous on the timescale of our experiments ($k_{5a} = 1.7 \times 10^7 - 1.7 \times 10^9 \text{ s}^{-1}$).

We have carried out a series of experiments on the detection of the probable products of IPN decomposition. Indeed, NO₂, CH₃ and acetaldehyde were directly detected as primary reaction products. Quantitative measurements were carried out at T = 610 K and P = 8.5 Torr and consisted in the monitoring of the concentrations of the products formed upon complete decomposition of IPN in the reactor. Experiments were carried out in the presence of relatively high concentration of Br₂ in the reactor ($[\text{Br}_2] \sim 5 \times 10^{13} \text{ molecule cm}^{-3}$) in order (i) to transform (via reaction 2) CH₃ radicals, once formed, into the stable species, CH₃Br, which can be easily and in an absolute way recorded with mass spectrometer and (ii) to avoid possible consumption of the radicals in secondary reactions. Initial concentration of IPN was varied in the range $(0.27 - 5.4) \times 10^{12} \text{ molecule cm}^{-3}$. The results of these experiments are shown in Figure 5.

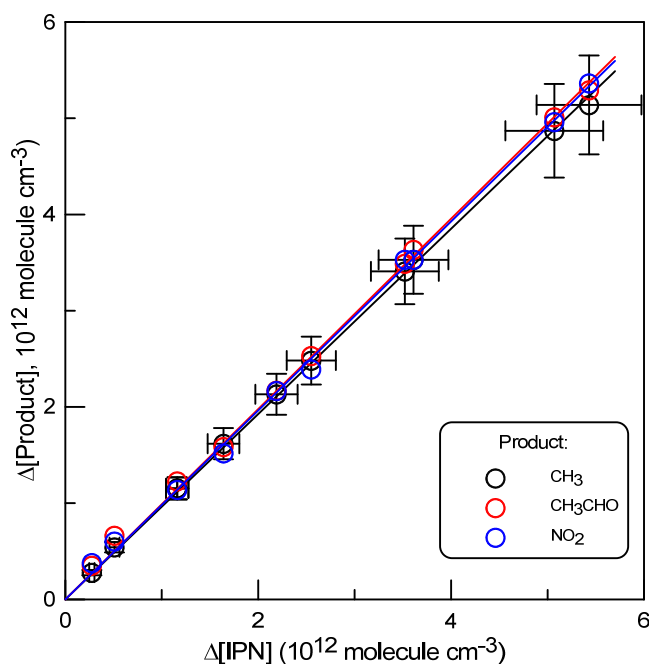


Figure 5. Concentration of the products formed upon decomposition of isopropyl nitrate as a function of consumed concentration of IPN: P = 8.5 Torr, T = 610 K. Error bars correspond to 10% uncertainty and reflect the precision of the measurements of the IPN and product concentrations.

The slopes of the straight lines in Figure 5 provide the yields of the corresponding species:

$$\Delta[\text{CH}_3]/\Delta[\text{IPN}] = 0.96 \pm 0.14,$$

$$\Delta[\text{NO}_2]/\Delta[\text{IPN}] = 0.98 \pm 0.15,$$

$$\Delta[\text{CH}_3\text{CHO}]/\Delta[\text{IPN}] = 0.99 \pm 0.15,$$

The estimated nearly 15% uncertainty on the measurements arises mainly from the combined errors on the measurements of the absolute concentrations of IPN and reaction products. These results confirm (i) the O–NO₂ bond cleavage as initial step of the mechanism of IPN decomposition and (ii) predominance of the (CH₃)₂CHO decomposition via C–C bond fission to CH₃ and acetaldehyde.

3.3. Rate constant of reaction (1) from kinetics of CH₃ formation. In this series of experiments, the rate constant of reaction (1) was determined in the temperature range 473 - 565 K from the kinetics of product formation under conditions where consumption of nitrate was negligible (less than 10% at highest temperature) and the rate constant could not be

determined from IPN decays. Under conditions where concentration of IPN is constant, the IPN decomposition product formation is governed by zeroth order kinetics:

$$d[\text{product}]/dt = k_1 \times [\text{IPN}] \quad (\text{IV})$$

and linear increase of product concentration with reaction time is expected. For these experiments, among three products of IPN decomposition we have chosen to follow CH_3 radical because mass spectra of NO_2 and acetaldehyde were highly perturbed by contribution of fragment peaks of IPN which was present in the reactor at relatively high concentrations. Br_2 was added in the reactor ($[\text{Br}_2] \sim 5 \times 10^{13} \text{ molecule cm}^{-3}$) in order to stoichiometrically convert CH_3 radicals to CH_3Br , which was monitored by mass spectrometry. Examples of kinetics of CH_3 production are shown in Figure 6.

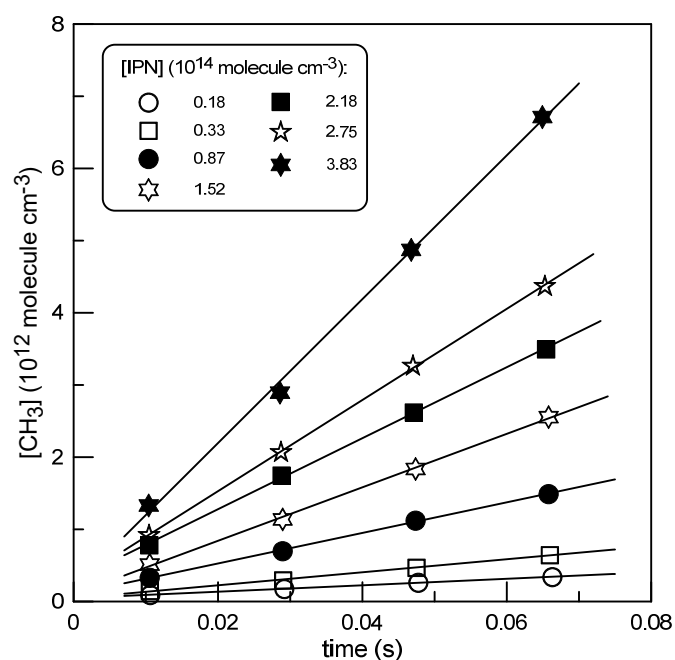


Figure 6. Kinetics of CH_3 production upon IPN decomposition recorded with different initial concentrations of IPN: $T = 528 \text{ K}$, $P = 4.4 \text{ Torr}$. Continuous lines represent linear fit to the experimental data.

The slopes of the straight lines in Figure 6 provide the rate of CH_3 production, $d[\text{CH}_3]/dt$ (in $\text{molecule cm}^{-3}\text{s}^{-1}$), which is presented in Figure 7 as a function of initial concentration of IPN.

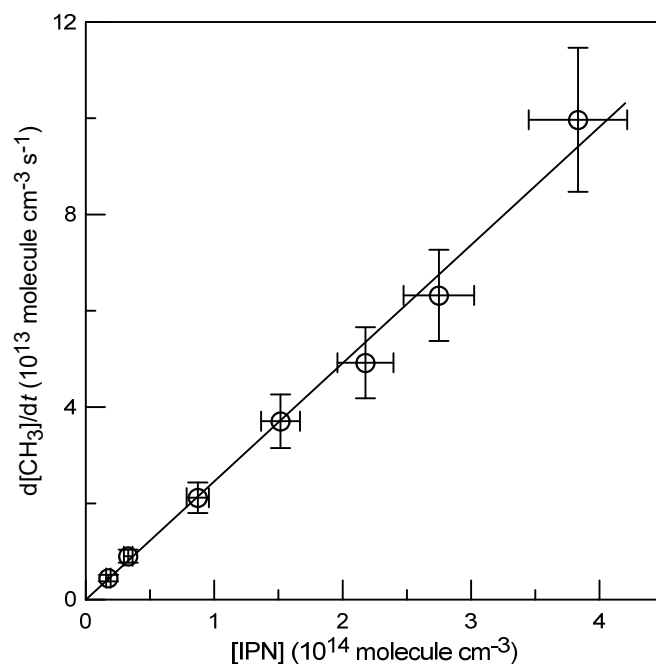


Figure 7. Rate of CH_3 production upon IPN decomposition as a function of concentration of isopropyl nitrate: $T = 528$ K, $P = 4.4$ Torr.

The observed linear, in accordance with equation (IV), dependence of $d[\text{CH}_3]/dt$ on $[\text{IPN}]$ (varied by a factor 20) indicates negligible contribution of possible secondary reactions which could lead to CH_3 production or consumption. The influence of the possible reaction of Br_2 with IPN (which is expected to be very slow) can also be ignored considering the following experimental observations: (i) addition of Br_2 into the reactor did not lead to any observable changes in the concentration of IPN, (ii) variation of Br_2 concentration in the range $(3 - 8) \times 10^{13}$ molecule cm^{-3} had no impact on the kinetics of CH_3 formation, and, finally, (iii) good agreement was observed between the values of the rate constant measured from CH_3 formation kinetics at $T = 565$ K and those of IPN decomposition measured at $T = 563$ K in Br_2 free system.

Example of kinetics of CH_3 production measured at $T = 524$ K and different pressures in the reactor is shown in Figure 2S (Supporting Information). The rate constant of reaction (1), calculated as $(1/[\text{IPN}]) \times d[\text{CH}_3]/dt$, is plotted in Figure 3S (Supporting Information) as a function of total pressure in the reactor. All the experimental data obtained for k_1 from the

kinetics of CH_3 production at different pressures and temperatures are shown in Figure 8. Procedure, similar to that used above in the case of IPN loss kinetics, was employed to extract low and high pressure limits of k_1 : continuous lines in Figure 8 represent the best fit to the experimental data according to equations (I) and (II) with $F_c = 0.6$ and two varied parameters, k_0 and k_∞ . The results obtained for k_0 and k_∞ in this series of experiments are presented in Table 1. Concerning the uncertainty on k_0 and k_∞ derived from the fit of falloff curves (with fixed value of $F_c = 0.6$) in Figures 4 and 8, it depends on the temperature of the measurements and has a different trend for low and high pressure limits of k_1 . For example, it is obvious that at lower temperatures (Figure 8), the simulated falloff curve is more sensible to the value of k_∞ and less to the value of k_0 , because k_1 is relatively close to its high pressure limit. To keep things simple, we place a conservative (nearly maximum) estimated uncertainty of a factor of 1.5 on all the derived values of k_0 and k_∞ . This uncertainty reflects the precision of the procedure of the falloff curve fitting taking into account uncertainties on the experimental data points.

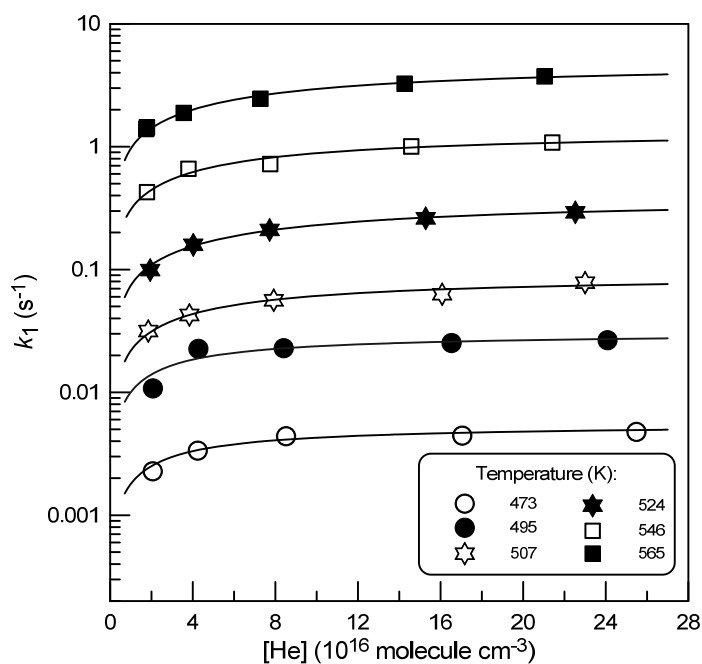


Figure 8. Rate constant of CH_3 production upon IPN decomposition as a function of total pressure of He at different temperatures in the reactor. Height of the symbols corresponds to nearly 15% uncertainty on k_1 .

3.4. Temperature dependence of k_1 . Temperature dependences of k_∞ and k_0 are demonstrated in Figures 9 and 10, respectively. One can note that the combination of two methods employed for the measurements of k_1 allowed the determination of the rate constant over a range of five orders of magnitude.

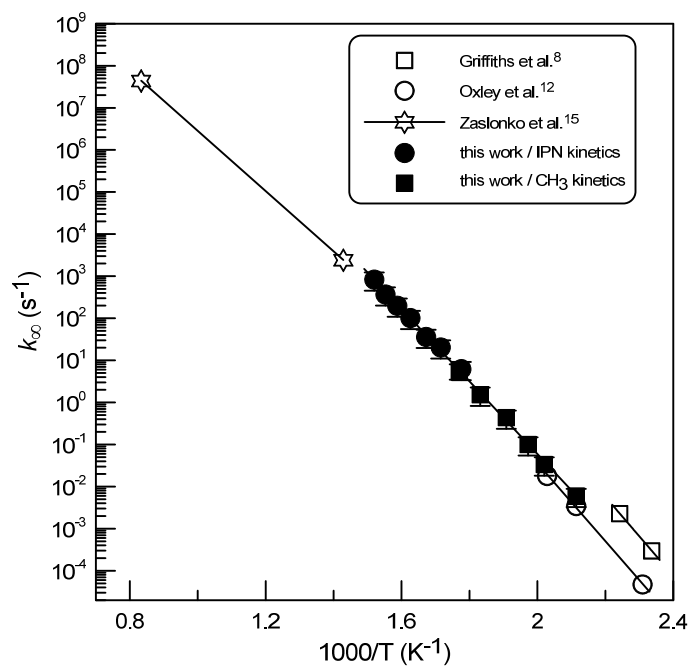


Figure 9. Temperature dependence of the high pressure limit of k_1 .

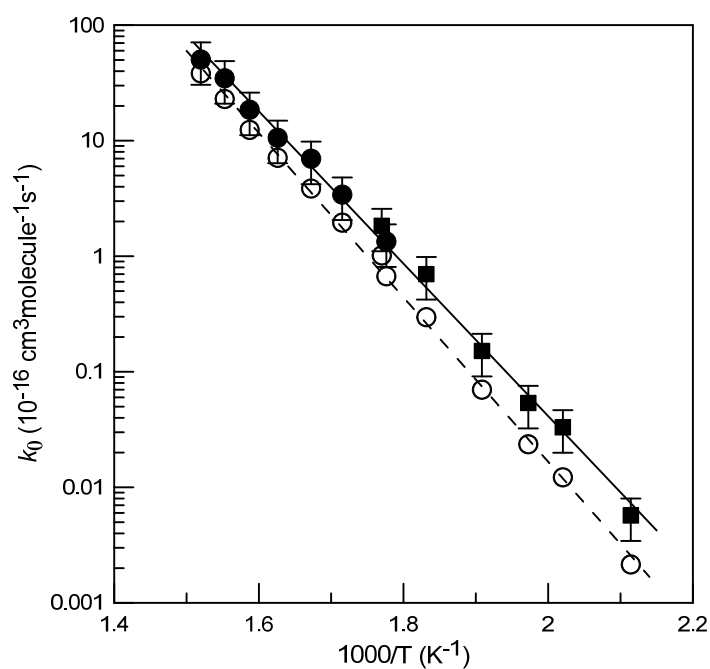


Figure 10. Temperature dependence of the low pressure limit of k_1 : data obtained from fit of the falloff curve according to equations (I) and (II) (filled symbols) and Lindemann-Hinshelwood expression (equation (I) with $F = 1$, open symbols).

Unweighted exponential fit to the experimental data in Figures 9 and 10 provides the following Arrhenius expressions:

$$k_{\infty} = 1.05 \times 10^{16} \exp(-19850/T) \text{ s}^{-1}$$

$$k_0 = 6.60 \times 10^{-5} \exp(-15190/T) \text{ cm}^3 \text{ molecule}^{-1} \text{ s}^{-1}$$

It should be emphasized again that the reported values of k_{∞} and k_0 depend on the choice of F_c -value used in the fitting of falloff curves and should be considered just as parameters allowing to represent the experimentally measured temperature and pressure dependence of the rate constant of IPN decomposition:

$$k_1 = \frac{k_0 k_{\infty} [M]}{k_0 [M] + k_{\infty}} \times 0.6^{(1 + (\log(\frac{k_0 [M]}{k_{\infty}}))^2)^{-1}}$$

This expression in combination with k_{∞} and k_0 given above reproduces all the temperature and pressure dependence data obtained for k_1 in the present study with accuracy within 20% and thus can be recommended for calculation of k_1 in the temperature range 473-658K and He pressures between 1 and 12.5 Torr with conservative uncertainty of 20%.

Concerning the possible use of the present data in combustion models, it seems that the expression for k_1 can be extrapolated to higher temperatures, of course, with increased uncertainty factor. Although the present measurements were realized with He as a bath gas, under combustion conditions (total pressure of 1 atm and higher) the rate constant of nitrate decomposition is expected to be close to high pressure limit, i.e. weakly dependent on the bath gas. We have shown that the primary step of the thermal decomposition of IPN is a cleavage of O-NO₂ bond. The distribution of other reaction products at combustion temperatures will depend on the fate of the isopropoxy radical. Estimations based on the

extrapolation of the available kinetic data for decomposition of $(\text{CH}_3)_2\text{CHO}^6$ and its reaction with O_2^{21} to high temperatures (1000 – 2000 K) indicate that decomposition (reaction 5) is the dominant loss process of isopropoxy radical in this temperature range.

As noted above the absolute values of k_∞ and k_0 determined in the present study depend on the F_c -value used in calculations. It seems to be interesting to compare the results obtained with $F_c = 0.6$ with those provided by data treatment using Lindemann-Hinshelwood expression (k_∞^{LH} and k_0^{LH}). The results obtained for k_∞ and k_0 within these two approaches are shown in Figures 4S (Supporting Information) and 10, respectively. Arrhenius fit to the experimental data (dashed lines in Figures 4S and 10) provides the following expressions for k_∞^{LH} and k_0^{LH} : $k_\infty^{\text{LH}} = 1.4 \times 10^{15} \exp(-18920/T) \text{ s}^{-1}$ and $k_0^{\text{LH}} = 2.8 \times 10^{-4} \exp(-16380/T) \text{ cm}^3 \text{ molecule}^{-1} \text{ s}^{-1}$. In the temperature range of the study, the ratios $k_\infty^{\text{LH}}/k_\infty$ and k_0^{LH}/k_0 are in the range (0.55 ÷ 0.95) and (0.34 ÷ 0.69), respectively. The corresponding difference in activation energies does not exceed 8%. Based on this comparison, it seems that the expressions for k_∞ and k_0 given above can be used as standalone with 10% uncertainty on the activation energies (39.3±4.0 and 30.1±3.0 kcal mol⁻¹, respectively) and, factor of 2 and 3 uncertainty on the respective preexponential factors.

To our knowledge, previously the rate of isopropyl nitrate decomposition was measured in a few studies.^{8,12,15} Griffiths et al.⁸ studying the decomposition of IPN in a static spherical Pyrex reactor (500 cm³) reported that over the limited temperature range 428-446 K the rate constant increased from 3.0×10^{-4} to $2.3 \times 10^{-3} \text{ s}^{-1}$ at total pressure of 22 Torr corresponding to the activation energy of ~ 42.8 kcal mol⁻¹. These two points are shown in Figure 9 together with the present data. Figure 9 shows also the results from Oxley et al.¹² for the rate of neat IPN decomposition in a liquid phase at temperatures between 433 and 493 K, with an exponential fit providing the following Arrhenius expression: $k_1 = 1.06 \times 10^{17} \exp(-21370/T) \text{ s}^{-1}$. Experiments with

different solvents and nitrate concentrations have not shown significant impact on k_1 .¹² Zaslanko et al.¹⁵ in their shock tube study reported the following expression for the rate of IPN decomposition in the temperature range 700 – 1200 K and total pressure 375 – 750 Torr of argon: $k_1 = 4.0 \times 10^{13} \exp(-16465/T) \text{ s}^{-1}$. The authors noted that under their experimental conditions the decomposition of nitrate occurred in the falloff regime. This makes it difficult to compare their results for k_1 with those for k_∞ from the present study and seems to be a probable reason for the relatively low activation energy measured in their study (32.6 kcal mol⁻¹). Even lower activation energy, 26.8 kcal mol⁻¹, was reported by Hansson et al.²² for IPN decomposition at temperatures 440-475 K and He pressure of nearly 200 Torr. One can note that the results of Oxley et al.¹⁴ are in fair agreement with those from the present work (Figure 9): in particular, the difference in activation energies from two studies is less than 10%.

The activation energy obtained in this study for k_∞ , $E_a = 39.3 \pm 4.0 \text{ kcal mol}^{-1}$, allows the determination of the O–NO₂ bond dissociation energy (BDE) in isopropyl nitrate as $\text{BDE} = E_a - RT_{\text{av}}$, where T_{av} is the average temperature of the T -range used in experiments:

$$\text{BDE (O-NO}_2) = 38.2 \pm 4.0 \text{ kcal mol}^{-1}.$$

This value is somewhat lower, although in agreement in the range of the quoted uncertainties with recommended by Luo,²³ $41.2 \pm 1.0 \text{ kcal mol}^{-1}$. Zeng et al.²⁴ using three density-functional methods calculated O–NO₂ bond dissociation energy of isopropyl nitrate. The BDE values computed with different DFT methods were in the range (33.8-41.7) kcal mol⁻¹, which overlaps the experimental value from this work. It seems that the extensive experimental data from the present study could serve as a basis to refine the theoretical approaches.

CONCLUSIONS

In this work, we investigated the kinetics and products of the thermal decomposition of isopropyl nitrate. The reaction rate constant was measured at $T = (473-658)$ K in the pressure range (1-12.5) Torr of helium. Primary product of the nitrate decomposition, NO_2 , was directly observed and its yield (nearly unity) was measured. The O- NO_2 bond dissociation energy was calculated to be in the range (38.2 ± 4.0) kcal mol⁻¹. The co-product of NO_2 , isopropoxy radical, was found to decompose instantaneously on the timescale of our experiments leading to exclusive production of CH_3 radical and acetaldehyde in the temperature range of the study.

ASSOCIATED CONTENT

Supporting Information.

Rate of IPN decomposition as a function of initial concentration of IPN (Figure 1S); kinetics of CH_3 formation upon IPN decomposition measured at different pressures in the reactor at $T = 524$ K (Figure 2S); rate constant of reaction (1), measured from kinetics of CH_3 production at $T = 524$ K, as a function of total pressure of He (Figure 3S); temperature dependence of the high pressure limit of k_1 : data obtained from fit of the falloff curves according to equations (II) and (III) and Lindemann-Hinshelwood expression (I) (Figure 4S). This material is available free of charge via the Internet at <http://pubs.acs.org>.

ACKNOWLEDGEMENT

This study was supported by French National Research Agency (ANR) through project ONCEM (12-BS06-0017-02). J. M. is very grateful for his PhD grant from CAPRYSES

project (ANR-11-LABX-006-01) funded by ANR through the PIA (Programme d'Investissement d'Avenir).

REFERENCES

- (1) Finlayson-Pitts, B. J.; Pitts, J. N. J., *Chemistry of the Upper and Lower Atmosphere: Theory, Experiments and Applications*. Academic Press: San Diego, 2000.
- (2) Clemitshaw, K. C.; Williams, J.; Rattigan, O. V.; Shallcross, D. E.; Law, K. S.; Anthony Cox, R. Gas-Phase Ultraviolet Absorption Cross-Sections and Atmospheric Lifetimes of Several C₂-C₅ Alkyl Nitrates. *J. Photochem. Photobio. A* **1997**, *102*, 117-126.
- (3) Clothier, P. Q. E.; Aguda, B. D.; Moise, A.; Pritchard, H. O. How Do Diesel-Fuel Ignition Improvers Work? *Chem. Soc. Rev.* **1993**, *22*, 101-108.
- (4) Inomata, T.; Griffiths, J. F.; Pappin, A. J. Twenty-Third Symposium (International) on Combustion. The Role of Additives as Sensitizers for the Spontaneous Ignition of Hydrocarbons. *Symp. Int. Combust.* **1991**, *23*, 1759-1766.
- (5) Toland, A.; Simmie, J. M. Ignition of Alkyl Nitrate/Oxygen/Argon Mixtures in Shock Waves and Comparisons with Alkanes and Amines. *Combust. Flame* **2003**, *132*, 556-564.
- (6) Curran, H. J. Rate Constant Estimation for C₁ to C₄ Alkyl and Alkoxy Radical Decomposition. *Int. J. Chem. Kinet.* **2006**, *38*, 250-275.
- (7) Adams, G. K.; Bawn, C. E. H. The Homogeneous Decomposition of Ethyl Nitrate. *Trans. Faraday Soc.* **1949**, *45*, 494-499.
- (8) Griffiths, J. F.; Gilligan, M. F.; Gray, P. Pyrolysis of Isopropyl Nitrate. I. Decomposition at Low Temperatures and Pressures. *Combust. Flame* **1975**, *24*, 11-19.
- (9) Houser, T. J.; Lee, B. M. H. Pyrolysis Kinetics of Ethyl Nitrate. *J. Phys. Chem.* **1967**, *71*, 3422-3426.
- (10) Levy, J. B. The Thermal Decomposition of Nitrate Esters. I. Ethyl Nitrate. *J. Am. Chem. Soc.* **1954**, *76*, 3254-3257.
- (11) Mendenhall, G. D.; Golden, D. M.; Benson, S. W. The Very-Low-Pressure Pyrolysis (VLPP) of n-Propyl Nitrate, tert-Butyl Nitrite, and Methyl Nitrite. Rate Constants for Some Alkoxy Radical Reactions. *Int. J. Chem. Kinet.* **1975**, *7*, 725-737.
- (12) Oxley, J. C.; Smith, J. L.; Rogers, E.; Ye, W.; Aradi, A. A.; Henly, T. J. Fuel Combustion Additives: A Study of Their Thermal Stabilities and Decomposition Pathways. *Energy Fuels* **2000**, *14*, 1252-1264.
- (13) Phillips, L. Thermal Decomposition of Organic Nitrates. *Nature* **1947**, *160*, 753-754.

- (14) Pollard, F. H.; Marshall, H. S. B.; Pedler, A. E. The Thermal Decomposition of Ethyl Nitrate. *Trans. Faraday Soc.* **1956**, *52*, 59-68.
- (15) Zaslanko, I. S.; Smirnov, V. N.; Tereza, A. M. High-Temperature Decomposition of Methyl, Ethyl, and Isopropyl Nitrates in Shock-Waves. *Kinet. Catal.* **1993**, *34*, 531-538.
- (16) Morin, J.; Romanias, M. N.; Bedjanian, Y. Experimental Study of the Reactions of OH Radicals with Propane, n-Pentane, and n-Heptane over a Wide Temperature Range. *Int. J. Chem. Kinet.* **2015**, *47*, 629-637.
- (17) Timonen, R. S.; Seetula, J. A.; Gutman, D. Kinetics of the Reactions of Alkyl Radicals (CH₃, C₂H₅, *i*-C₃H₇, and *t*-C₄H₉) with Molecular Bromine. *J. Phys. Chem.* **1990**, *94*, 3005-3008.
- (18) Troe, J. Toward a Quantitative Analysis of Association Reactions in the Atmosphere. *Chem. Rev.* **2003**, *103*, 4565-4576.
- (19) Troe, J. Predictive Possibilities of Unimolecular Rate Theory. *J. Phys. Chem.* **1979**, *83*, 114-126.
- (20) J. B. Burkholder, S. P. S., J. Abbatt, J. R. Barker, R. E. Huie, C. E. Kolb, M. J. Kurylo, V. L. Orkin, D. M. Wilmoth, P. H. Wine. Chemical Kinetics and Photochemical Data for Use in Atmospheric Studies, Evaluation No. 18. JPL Publication 15-10, Jet Propulsion Laboratory: Pasadena, 2015 <http://jpldataeval.jpl.nasa.gov>.
- (21) Atkinson, R. Atmospheric Reactions of Alkoxy and B-Hydroxyalkoxy Radicals. *Int. J. Chem. Kinet.* **1997**, *29*, 99-111.
- (22) Hansson, T.; Pettersson, J. B. C.; Holmlid, L. A Molecular Beam Mass-Spectrometric Study of Isopropyl Nitrate Pyrolysis Reactions at Short Residence Times and Temperatures up to 700 K. *J. Chem. Soc., Faraday Trans. 2* **1989**, *85*, 1413-1423.
- (23) Luo, Y. R., *Handbook of Bond Dissociation Energies in Organic Compounds*. CRC Press: Boca Raton, FL, 2003.
- (24) Zeng, X.-L.; Chen, W.-H.; Liu, J.-C.; Kan, J.-L. A Theoretical Study of Five Nitrates: Electronic Structure and Bond Dissociation Energies. *J. Mol. Struct. - THEOCHEM* **2007**, *810*, 47-51.

TABLE OF CONTENT IMAGE

